

ASSESSING THE EFFECTIVENESS OF A NSM-CFRP FLEXURAL STRENGTHENING ARRANGEMENTS FOR CONTINUOUS RC SLABS BY EXPERIMENTAL AND NUMERICAL RESEARCH

Gláucia DALFRÉ

Professor, Federal University of the Latin American Integration (UNILA), Brazil
glaucia.dalfré@unila.edu.br

Joaquim BARROS

Full Professor, University of Minho, Portugal
barros@civil.uminho.pt

ABSTRACT: A program formed by continuous slab strips strengthened in flexure with near surface mounted (NSM) Carbon Fiber Reinforced Polymer (CFRP) laminates was carried out, and the obtained results showed the possibility of increasing significantly the load carrying capacity of these elements, maintaining high levels of ductility. The experimental program is formed by slab strips of two equal span lengths, and has the main purpose of exploring the potentialities of distinct NSM flexural strengthening configurations for the increase of the load carrying capacity of this type of structures. In the present work two types of strengthening arrangements were investigated, one with CFRP laminates exclusively applied at the intermediate support, H series (hogging region), and the other with laminates applied at both hogging and sagging regions (HS series). For assessing the predictive performance of a FEM-based computer program (FEMIX V4.0), the experimental results are compared with values predicted by this software. Then, a parametric study with 144 numerical models is carried out to investigate the influence of the strengthening arrangement and CFRP percentage in terms of moment redistribution and rotational capacities of continuous RC slab strips flexurally strengthened by the NSM technique. The obtained results are presented and analyzed in this paper.

1. Introduction

In general, when a structural Reinforced Concrete (RC) element is strengthened with fiber reinforced polymer (FRP) systems its failure mode tends to be more brittle than its unstrengthened homologous element, due to the intrinsic bond conditions between these systems and the concrete substrata, as well as the linear-elastic brittle tensile behavior of FRPs. In case of continuous RC slabs and beams (statically indeterminate structures), the use of FRP systems to increase their flexural resistance can even compromise the moment redistribution capacity of these types of elements. Thus, to contribute for a better understanding the influence of the strengthening arrangement (hogging, sagging or both regions) and percentage of FRP in terms of load carrying capacity, moment redistribution capacity and ductility performance, a parametric study was carried out. This parametric study was performed by executing material nonlinear analysis with a computer program based on the Finite Element Method (FEM), whose predictive performance was appraised with the results obtained in experimental programs (Bonaldo 2008 and Dalfré 2013).

2. Numerical simulations and parametric study

The reliability of this study requires the use of a computational tool capable of simulating the relevant aspects of this structural system. For this purpose, the version 4.0 of FEMIX computer program was used. FEMIX 4.0 is a computer code whose purpose is the analysis of structures by the Finite Element Method (FEM). In this study, at first, the tests of the experimental programs with statically indeterminate slab strips carried out by Bonaldo (2008) and Dalfré (2013) were simulated, and a good predictive performance was obtained. Thus, a parametric study for the evaluation of the influence of relevant parameters on the moment redistribution level and ductility performance of statically indeterminate RC slabs strengthened according to the NSM technique was executed. These parameters are: concrete strength class, percentage of existing longitudinal tensile reinforcement, strengthening configuration, and percentage of CFRP laminates.

2.1. Mechanical properties of the intervenient materials and strengthening arrangements

In the parametric study, the mechanical properties adopted for the concrete strength classes (C12/15, C25/30 or C35/45) were determined following the recommendations of Eurocode 2 (2010) and CEB-FIP Model Code (1993), which are presented in Table 1. The values of the parameters adopted for the constitutive model used to simulate the behaviour of the steel bars are those included in Table 2. The arrangements of the steel reinforcement, dimensions of the cross section, support and load conditions are the same adopted in the experimental/numerical program for the reference slab strip of SL15-H/HS series tested by Bonaldo (2008) and Dalfré (2013). However, distinct strengthening arrangements and bond lengths were applied in the hogging (H) and sagging regions (S), as shown in Figure 1.

Table 1 - Concrete properties used for the FEM simulations

Parameters	C12/15	C25/30	C35/45
Compressive strength (N/mm ²)	$f_{cm} = 20$	$f_{cm} = 33$	$f_{cm} = 43$
Initial Young's modulus (N/mm ²)	$E_c = 22.85$	$E_c = 27.21$	$E_c = 30.82$
Poisson's ratio	$\nu_c = 0.00$		
Strain at compressive strength	$\epsilon_{c1} = 2.80 \times 10^{-3}$	$\epsilon_{c1} = 2.80 \times 10^{-3}$	$\epsilon_{c1} = 2.80 \times 10^{-3}$
Tri-linear tension softening ⁽¹⁾	$f_{ct} = 1.10$ N/mm ² $G_f = 0.041$ N/mm	$f_{ct} = 1.75$ N/mm ² $G_f = 0.058$ N/mm	$f_{ct} = 2.14$ N/mm ² $G_f = 0.070$ N/mm
	$\xi_1 = 0.015; \alpha_1 = 0.6; \xi_2 = 0.2; \alpha_2 = 0.25$		
Parameter defining the initial yield surface	$\alpha_0 = 0.4$		
Parameter defining the mode I fracture energy to the new crack	$n = 2$		
Parameter to define the evolution of the shear retention factor	$p_1 = 2$		
Crack band-width	Square root of the area of Gauss integration point		
Threshold angle	$\alpha_{th} = 30^\circ$		
Maximum numbers of cracks per integration point	2		

⁽¹⁾ $f_{ct} = \sigma_{n,1}^{cr}$; $\xi_1 = \epsilon_{n,2}^{cr} / \epsilon_{n,u}^{cr}$; $\alpha_1 = \sigma_{n,2}^{cr} / \sigma_{n,1}^{cr}$; $\xi_2 = \epsilon_{n,3}^{cr} / \epsilon_{n,u}^{cr}$; $\alpha_2 = \sigma_{n,3}^{cr} / \sigma_{n,1}^{cr}$ (Sena-Cruz, 2004); Eurocode 2 (2010); CEB-FIP Model Code (1993).

Table 2 - Values of the parameters of the steel constitutive model

Steel bar diameter	$P_1(\epsilon_{sy}[-]; \sigma_{sy}[\text{MPa}])$	$P_2(\epsilon_{sh}[-]; \sigma_{sh}[\text{MPa}])$	$P_3(\epsilon_{su}[-]; \sigma_{su}[\text{MPa}])$	E_s [GPa]
Ø 8mm	(1.90×10^{-3} ; 379.16)	(4.42×10^{-2} ; 512.19)	(8.85×10^{-2} ; 541.66)	200.80
Ø 10mm	(2.32×10^{-3} ; 413.20)	(3.07×10^{-2} ; 434.75)	(1.31×10^{-1} ; 546.25)	178.23
Ø 12mm	(2.09×10^{-3} ; 414.35)	(3.05×10^{-2} ; 435.63)	(1.02×10^{-1} ; 537.98)	198.36

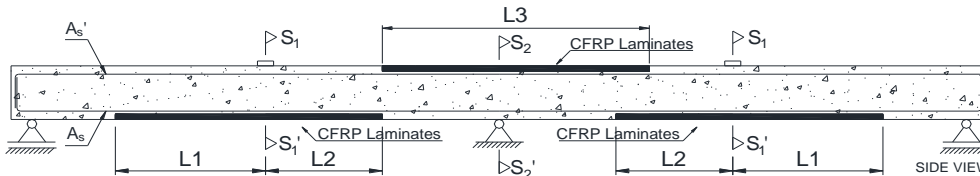


Fig. 1 - Length of the NSM CFRP laminates for the slab strips

3. Results and discussion

The slab strips can be classified in three different groups, due to the distinct adopted strengthening arrangements: (a) applied in the hogging region, (b) applied in the sagging regions and (c) applied in both hogging and sagging regions. The notation adopted to identify a slab strip is SLx_y_w_z, where x is the moment redistribution percentage, η (15%, 30% and 45%), y is the concrete strength class (C12/15, C25/30 or C35/45), and w and z indicate the number of NSM CFRP laminates applied in the sagging or hogging regions, respectively. Therefore, SL15_30_4_2 represents a slab with a moment redistribution target of $\eta = 15\%$, made by

a concrete of $f_{ck} = 30$ MPa (in cubic specimens), and strengthened with 4 and 2 laminates in the sagging and hogging regions, respectively. In the numerical simulations, the analyses were assumed ended when one of the following two considered failure conditions was attained: (i) when the concrete crushing strain was reached in the sagging region ($\varepsilon_c^S = 3.5\%$); (ii) when the effective strain in the CFRP laminates, ε_{fd} , was attained in the sagging or in the hogging region. This ε_{fd} is the maximum tensile strain that can be applied in order to prevent a failure controlled by FRP debonding, also designated by effective failure strain. According to the ACI 440 (2008), for NSM FRP applications $\varepsilon_{fd} = 0.7\varepsilon_{fu}$, where ε_{fu} is the ultimate strain obtained from uniaxial tensile tests. Due to the limited space, only the results concerning to the SL15 Series are represented, but similar behavior was obtained for all the Series. The entire parametric study is treated in detail elsewhere (Dalfré, 2013). The rotational ductility index (μ_χ) and the moment redistribution index (*MRI*) of the hogging ($\rho_{s,eq}^H$) and sagging ($\rho_{s,eq}^S$) regions are presented, where $\rho_{s,eq} = A_s / (bd_s) + (A_f E_f / E_s) / (bd_f)$ is the percentage of equivalent steel reinforcement (equivalent reinforcement ratio), where b is the width of the slab's cross section and d_s and d_f are the effective depth of the longitudinal steel bars and CFRP laminates, respectively, and E_s and E_f are the Young's modulus of the longitudinal tensile steel bars and CFRP laminates. Additionally, ρ_f^H and ρ_f^S are the percentage of CFRP laminates in the hogging [$\rho_f^S = A_f^S / (bd_f^S)$] and sagging regions [$\rho_f^H = A_f^H / (bd_f^H)$], respectively.

3.1. Rotational ductility index

The rotational ductility (ν) is defined as the ratio between the curvatures of the loaded section at the formation of the second and the first hinges ($\nu = \chi_{2nd} / \chi_{1st}$). The rotational ductility index (μ_χ) is expressed as the ratio between the rotational ductility of the strengthened (ν_{streng}) and the reference (ν_{ref}) slab strips ($\mu_\chi = \nu_{streng} / \nu_{ref}$). The relationships $\mu_\chi - \rho_{s,eq}^S$ and $\mu_\chi - \rho_{s,eq}^H$ are represented in Fig. 2. In this figures it is also indicated the relationships $\mu_\chi - \rho_f^S$ and $\mu_\chi - \rho_f^H$. The rotational ductility decreases with the increase of the percentage of the CFRP laminates in the hogging region. In fact, values of μ_χ smaller than 1 were obtained for some strengthening configurations, which means that these configurations have a detrimental influence in terms of rotational ductility performance. Also, the rotational ductility decreases with ρ_f^S , and values of μ_χ higher than 1 are obtained for the configurations with $\rho_f^H = 0$. In the slab strips strengthened in both sagging and hogging regions, $\mu_\chi < 1$, which means that the strengthened sections slab have a considerable lower rotational capacity than the corresponding sections of its reference slab.

3.2. Moment redistribution index

The moment redistribution index (*MRI*) is defined as the ratio between the η of a strengthened slab, η_{streng} , and the η of its reference slab, η_{ref} , ($MRI = \eta_{streng} / \eta_{ref}$), where η is the moment redistribution percentage at the formation of the second hinge (in the sagging region). The relationships $MRI - \rho_{s,eq}^S$ and $MRI - \rho_{s,eq}^H$ obtained in the numerical simulations for the three concrete strength classes are shown in Fig. 3. In this figure it is also indicated the relationships $MRI - \rho_f^S$ and $MRI - \rho_f^H$. It is observed that the *MRI* depends strongly on the strengthening arrangement. In the slab strips only strengthened in the hogging region η_{streng} is less than η_{ref} . Increasing the percentage of laminates in the sagging region, *MRI* increases, regardless the $\rho_{s,eq}^H$. For slabs only strengthened in the sagging regions, $MRI > 1.0$, which means that this type of slabs has higher moment redistribution capacity than its reference slab. However, with the increase of the percentage of laminates in the hogging region the *MRI* decreases. Fig. 3 also shows a good agreement between the results of the parametric study and the values obtained in the experimental programs described in Bonaldo (2008) and Dalfré (2013). To avoid a decrease in the moment redistribution capacity, CFRP laminates strips should be applied in both sagging and hogging regions, in appropriate percentages. Fig. 4 shows that the moment redistribution index increases with $\rho_{s,eq}^S / \rho_{s,eq}^H$. For $\rho_{s,eq}^S / \rho_{s,eq}^H > 1.09$ the *MRI* is positive for η equal to 15%.

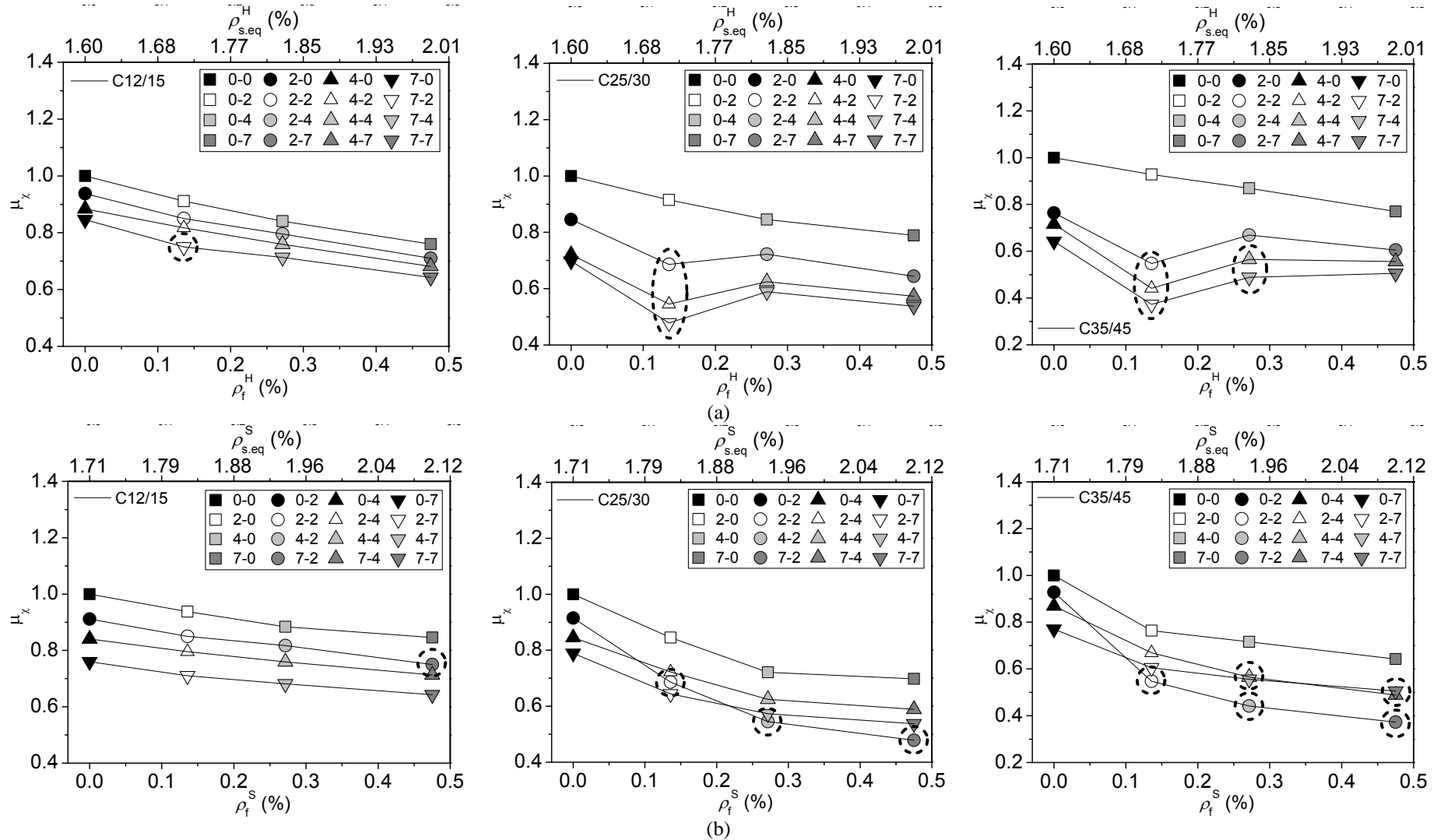


Fig. 2 - Relationship between the rotational ductility index, μ_x , and the CFRP strengthening ratio/equivalent reinforcement ratio in the (a) hogging and (b) sagging regions for the SL15 Series.

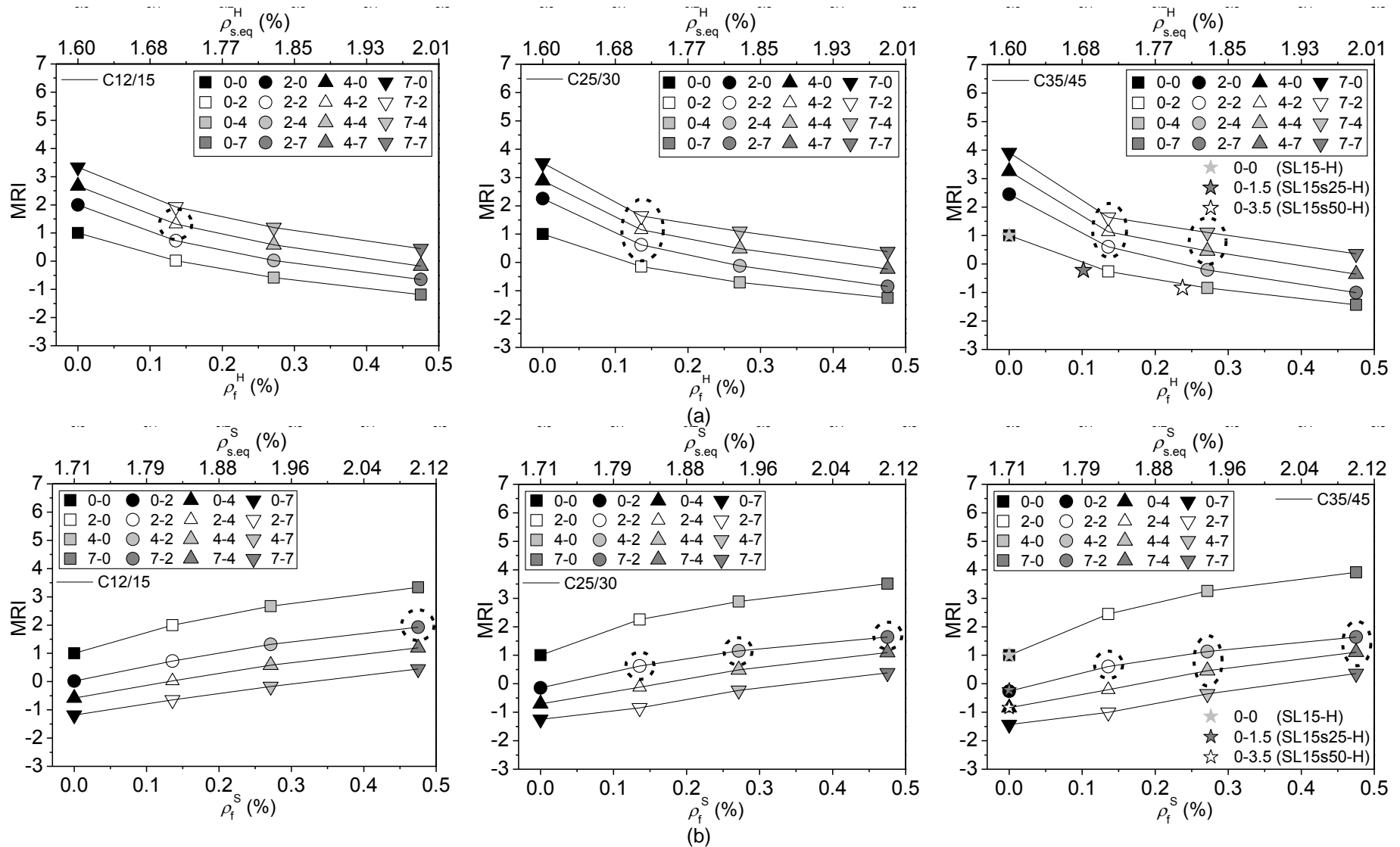


Fig. 3 - Relationship between the moment redistribution index, MRI, and the CFRP strengthening ratio/equivalent reinforcement ratio in the (a) hogging and (b) sagging regions for the SL15 Series.

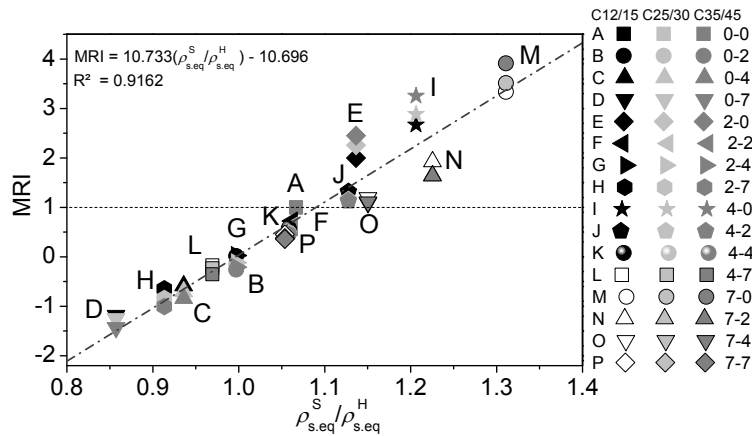


Fig. 4 - Relationship between the moment redistribution index and $\rho_{s,eq}^S / \rho_{s,eq}^H$ for the SL15 series.

4. Conclusions

To evaluate the influence of the concrete strength class, the percentage of existing longitudinal tensile reinforcement and the percentage of CFRP on the strengthening effectiveness, moment redistribution capacity and ductility performance, a parametric study was carried out by executing material nonlinear analysis with a FEM-based computer program, which predictive performance was calibrated using the results of the experimental programs performed by Bonaldo (2008) and Dalfré (2013). From the obtained results it can be pointed out the following main observations: (i) The moment redistribution and the rotational capacities are strongly depend on the flexural strengthening arrangement; (ii) The moment redistribution decreases with the increase of $\rho_{s,eq}^H$ and increases with $\rho_{s,eq}^S$, where $\rho_{s,eq} = A_{sl} / bd_s + (A_f E_f / E_s) / (bd_f)$ is the equivalent reinforcement ratio; (iii) The moment redistribution increases with $\rho_{s,eq}^S / \rho_{s,eq}^H$ and positive values (which means that the moment redistribution of the strengthened slab is higher than its corresponding reference slab) are positive when $\rho_{s,eq}^S / \rho_{s,eq}^H > 1.09$. Additionally, when considering all the series analysed in this work, a good fit for a linear model was obtained for $\eta - \rho_{s,eq}^S / \rho_{s,eq}^H$. Thus, the moment redistribution percentage can be estimated by using the parameter $\rho_{s,eq}^S / \rho_{s,eq}^H$; (iv) The rotational capacity of the strengthened slab strips decreases with the increase of $\rho_{s,eq}^H$, and increases with $\rho_{s,eq}^S$. In the slab strips strengthened in both sagging and hogging regions, a rotational capacity lower than its reference slabs was obtained. In conclusion, the obtained results evidence that the use of efficient strengthening strategies can provide adequate level of ductility and moment redistribution in statically indeterminate structures.

5. Acknowledgements

The first author acknowledges the financial support of FCT (PhD Grant number SFRH/BD/69818/2010) and the National Council for Scientific and Technological Development (CNPq) – Brazil (GDE 200953/2007-9).

6. References

- Everaldo Bonaldo, "Composite materials and discrete steel fibres for the strengthening of thin concrete structures", *PhD Thesis*, University of Minho, Guimarães, Portugal, 2008.
- CEB-FIP Model Code 1990, "Design Code", *Thomas Telford*, Lausanne, Switzerland, 1993.
- Gláucia Dalfré, "Flexural and shear strengthening of RC element", *PhD Thesis*, University of Minho, Portugal, 2013.
- EN 1992-1-1, "Eurocode 2: Design of Concrete Structures-Part 1-1: General Rules and Rules for Buildings", *CEN*, Brussels, 2010.
- José Manuel de Sena-Cruz, "Strengthening of concrete structures with near-surface mounted CFRP laminate strips", *PhD Thesis*, Department of Civil Engineering, University of Minho, Portugal, 2004.